Polymer Bulletin (2019) 76:3785–3801
https://doi.org/10.1007/s00289-018-2569-6

ORIGINAL PAPER

Cyclotriphosphazene nanofiber-reinforced polybenzoxazine/epoxy nanocomposites for low dielectric and flame-retardant applications

M. Selvi[1] · S. Devaraju[2] · M. Alagar[3]

Received: 1 July 2017 / Revised: 17 September 2018 / Accepted: 15 October 2018 /
Published online: 27 October 2018

Abstract

In the present work, a halogen-free flame-retardant cyclotriphosphazene nanofiber-reinforced polybenzoxazine/epoxy (PBZ/EP/PZT) hybrid nanocomposites have been developed and characterized. Initially, equimolar quantities of benzoxazine and the epoxy matrix is blended and varying weight percentages (0, 0.5, 1.0 and 1.5 wt%) of PZT nanofiber are reinforced to obtain hybrid nanocomposites. It was observed that PBZ/EP/PZT nanocomposites possess higher values of glass transition temperatures (T_g—208 °C) and displayed enhanced thermal stability with high char yields than those of neat matrix. The flammability characteristics of the nanocomposites were studied on the basis of the LOI, UL-94 burning experiments as well as the analysis of residual chars of the tested bars after burning. The V-0 classification for the nanocomposites indicates that the incorporation of PZT nanofiber (1.5 wt%) imparts enhanced flame retardancy to the PBZ/EP matrix. The dielectric properties of these nanocomposites have been studied at 1 MHz over the temperature range between 30 and 200 °C. Data resulted from thermal, flame-retardant and dielectric studies indicate that the composite materials can be considered as the potential candidate for thermally stable fire and heat resistant, dielectric sealants, and encapsulants in electronic applications.

Keywords Benzoxazine · Epoxy · Cyclotriphosphazene nanofibers · Thermal stability · Flame retardant · Dielectric constant

✉ S. Devaraju
subudeva@gmail.com

✉ M. Alagar
mkalagar@yahoo.com

Extended author information available on the last page of the article

Introduction

The use of polymeric materials in a day-to-day life is increasing due to their remarkable combination of properties, varying range of molecular weight and ease of processing. However, polymers are also known for their relatively high flammability; most often accompanied by the evolution of corrosive or toxic gases and smoke during burning. Consequently, improving the fire-retardant behavior of polymers is a major challenge for extending their use to most high-performance industrial applications [1–3].

Epoxy resin is one of the most important thermoset engineering polymers with a wide range of industrial applications, such as packaging, adhesives, encapsulating materials for electronics, coatings, aerospace and marine systems because of their good chemical resistance, excellent thermal and electrical insulating properties, and high tensile strength [4–9]. However, the neat epoxy resin is highly flammable, which significantly restricts its applications. Therefore, the modification of epoxy in order to improve its flame retardancy is an important issue and needs to be addressed. Generally, there are several approaches to reduce the polymer flammability, i.e., (1) to use the inherently flame-retarded polymers (polyimide, polybenzoxazine, etc.,) [10], (2) to chemically modify the existing polymers (copolymerization of flame-retardant monomers into the polymer chains) [11]; and (3) to incorporate flame retardants into the hosting polymer matrix [12–18]. All these methods could be used for enhancing the flame retardancy of epoxy resin. Because inherently flame-retardant polymers can lead to high production costs, the modification of already existing systems is still valued by industries. As thermally stable materials, polybenzoxazines possess good flame-retardant behavior and are useful for electronic and aerospace applications as sealant and coating materials. Benzoxazine resins can be easily synthesized from phenol, formaldehyde, and amine through Mannich reaction by either solution or bulk method. The polymerization of resins proceeds via ring opening of oxazine rings by a thermal cure. On curing, benzoxazine resins develop a phenolic-like structure with inherent flame-retardant properties. Polybenzoxazines exhibit the characteristics that found in traditional phenolic such as heat resistance, flame retardance, and good electrical insulation behavior. Besides, they also exhibit lots of unique characteristics including low melt viscosity, dimensional stability, excellent mechanical properties, as well as low water absorption [19–25]. Even though having aromatic bisphenol and the aromatic diamine as raw materials, the resultant polybenzoxazines do not possess enough flame retardancy for electronic materials where a flame retardancy of the UL-94 grade is required. Hence, the incorporation of flame-retardant materials in polymers is still widely used. It is considered as a simple and cost-effective method for preparing flame-retarding polymers.

Phosphazenes, particularly polyphosphazenes, are a well-known class of versatile functional materials having an inorganic backbone structure. The compounds containing both phosphorus and nitrogen are expected to display enhanced flame retardancy when compared to that of similar compounds containing phosphorus alone. The reason is that the thermal decomposition of the phosphazene-based

polymers is an endothermic process, and phosphate, metaphosphate, poly-phosphate generated in the thermal decomposition form a non-volatile protective film on the surface of the polymer to isolate it from the air; meanwhile, the inflammable gases released such as CO_2, NH_3, and N_2 cut off the supply of oxygen and contribute to the synergistic flame-retardant behavior. The properties of organic polymers can be modified significantly to improve their fire resistance, ionic conductivity, biological compatibility, or other properties by the incorporation of a small amount of a specifically tailored phosphazene. This makes phosphazenes particularly good candidates for the development of fire-resistant materials for use in electric and electronic applications [26–34]. Only a few of the researcher worked with phosphazene fiber-reinforced polymer composites for flame resistant applications. Here, the cyclophosphazene nanofiber/sphere with the unique combination of phosphorus and nitrogen contributes to imparting the good flame-retardant behavior of the resulting polymer composites [31–34].

In the present work, an attempt has been made to develop non-flammable halogen-free hybrid nanocomposites based on polybenzoxazine/epoxy (PBZ/EP) matrix by reinforcing with PZT nanofiber, and their thermal, flame-retardant, and dielectric properties were studied and discussed. As the data results, 1.0% PZT-reinforced PBZ/EP/PZT nanocomposites possess V-0 classification (UL-94 test), indicating an excellent flame-retardant behavior.

Experimental

Materials

Hexachlorocyclotriphosphazene (HCCP) and 4,4′-sulfonyldiphenol (BPS) were purchased from Sigma-Aldrich, India. The epoxy resin (diglycidyl ether of bisphenol-A, DGEBA) was supplied by Ciba-Geigy Ltd., India. Bisphenol-A, aniline, paraformaldehyde, tetrahydrofuran (THF), triethylamine (TEA), and methanol were received from SRL (India) Ltd. Bisphenol-A/aniline-based benzoxazine (Bz) was synthesized as per reported procedure [22].

Characterizations and techniques

FTIR spectra were recorded on a PerkinElmer 6X spectrometer. About 500 mg of optical-grade KBr was ground in a mortar with a pestle, and enough amount of solid sample was ground with KBr to make 1 wt% mixture for making KBr pellets. After the sample was loaded, a minimum of 16 scans were collected for each sample at a resolution of ± 4 cm^{-1}. The DSC was performed on a NETZSCH DSC-200PC (TA instruments USA) with a heating rate of 10 °C/min, the measurements were taken from 30 to 300 °C under nitrogen atmosphere (20 mL/min). The instrument was calibrated with indium supplied by NETZSCH. About 10 mg of the samples was taken for each analysis. Thermogravimetric analysis was performed in TGA-Thermal Analyst NETZSCH STA 409PC (TA instruments USA) at a heating rate of

20 °C/min from 30 to 800 °C under a continuous flow of nitrogen (20 mL/min). The instrument was calibrated with the help of calcium oxalate and aluminum supplied by NETZSCH. About 10 mg of the samples was taken for each analysis. The dielectric constant and dielectric loss of the polybenzoxazine systems (length, width, and thickness of the sample specimen 10mmX10mmX3 mm, respectively) were determined with the help of an impedance analyzer (Solartron impedance/gain-phase analyzer 1260) using a platinum (Pt) electrode at 1 MHz at a temperature range of 30 °C to 200 °C. This experiment was repeated four times under the same conditions. The UL-94 vertical burning test was carried out for the PBZ/EP/PZT based on the testing method proposed by Underwriter Laboratory according to ASTM D-1356 standard. The SEM morphology of the residual chars was performed using a JEOL JSM Model 6360 microscope. The char residues of the specimen were coated with gold and were exposed to an accelerating voltage of 20 kV. A JEOL JEM-3010 analytical transmission electron microscope, operating at 300 kV with a measured point-to-point resolution of 0.23 nm, was used to characterize the phase morphology of the polymers.

Synthesis of the sulfone-containing phosphazene nanotubes (PZT)

The required stoichiometric quantity of HCCP and BPS as per the procedure reported in the literature [35] was charged to yield PZTs containing active hydroxyl groups: 8.73 g of triethylamine (0.0862 mol) was added to a solution of HCCP (5 g, 0.0143 mol) and BPS (14.4 g, 0.0575 mmol) in THF (100 mL). The reaction mixture was kept in an ultrasonic bath (100 W, 80 kHz) at 30 °C for 6 h. The product resulted was filtrated and then washed three times with THF and deionized water. The filtered solid was dried in a vacuum oven, and the sample PZT was obtained as white powder (Scheme 1).

Development of PBZ/EP/PZT nanocomposites

PZT fiber of 0, 0.5, 1.0, and 1.5 wt% was reinforced with PBZ/EP (1:1 weight ratio) in THF solvent and stirred for 12 h at 30 °C. After 12 h, the resultant PBZ/EP/PZT hybrid nanocomposite samples were separately cast on a smooth glass substrate and thermally treated at 50 °C for 1 day, and at 80, 100, 120, 140, 160, 180, 200 for 1 h each and 220 °C for 2 h. The light brown-colored films formed were stripped from the glass substrates, and then they are utilized for further characterization (Scheme 2).

Results and discussion

Halogenated flame-retardant materials are usually incorporated into the polymer matrix to improve its flame-retardant performance, whereas these materials release toxic gases and corrosive smoke during combustion; hence, it results in unwarranted environmental concerns. Accordingly, the development of non-halogenated

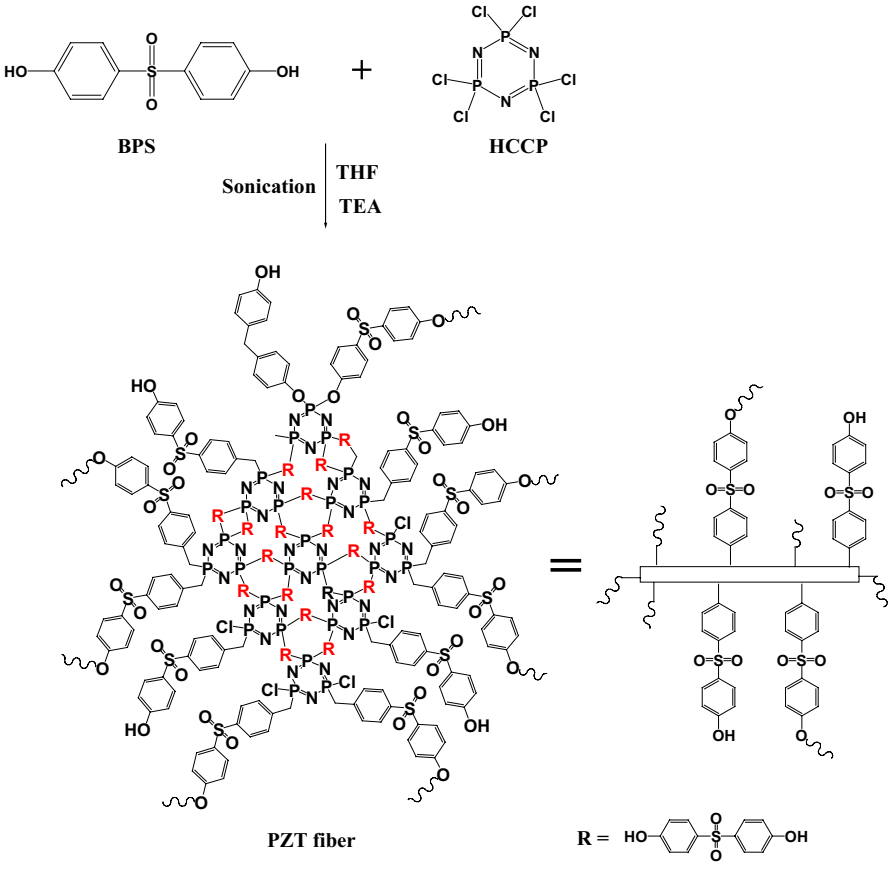

Scheme 1 Synthesis of sulfone-containing phosphazene fiber (PZT)

flame-retardant system becomes an attractive and emergent subject [36]. As an alternative to halogenated flame retardants, phosphorus-based flame retardants are expected to play a major role, [8, 37, 38] because phosphorus can act in the condensed phase promoting char formation on the surface, which acts as a barrier to inhibit gaseous products from diffusing to the flame and to shield the polymer surface from heat and air. Nitrogen-containing compounds are another class of halogen-free flame retardants which can release non-flammable gases or decompose endothermically to cool the pyrolysis zone at the combustion surface. An incorporation of these phosphorus- and nitrogen-containing phosphazene fiber into PBZ/EP matrix by the chemical method, which contributes to improved flame retardancy. The introduction of cyclotriphosphazene moieties into the backbone is expected to enhance the thermal resistance, thermal stability, and most importantly, the fire resistance of the resulting PBZ/EP matrix.

The FTIR spectra of neat PBZ/EP and PBZ/EP/PZT are shown in Fig. 1. The stretching bands at 1234, 1178, and 823 cm^{-1} correspond to the P=N and P–N

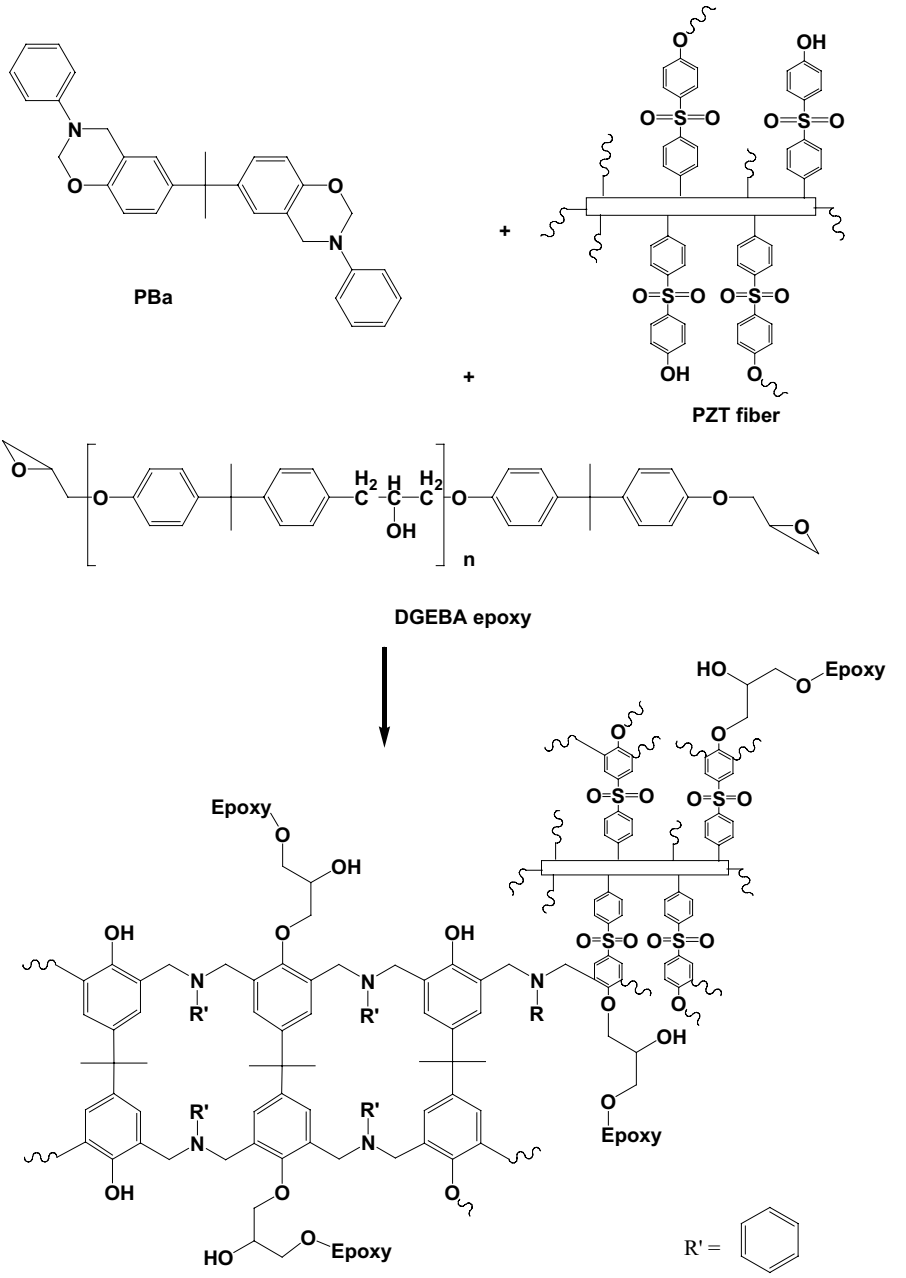

Scheme 2 Schematic representation of PBZ/EP/PZT nanocomposites

characteristic absorption; the characteristic peaks appeared at 1358, 1290, and 1105 cm^{-1} are assigned to O=S=O; 1591 and 1496 cm^{-1} correspond to C=C absorption; the intense absorption appeared at 941 cm^{-1} corresponds to the

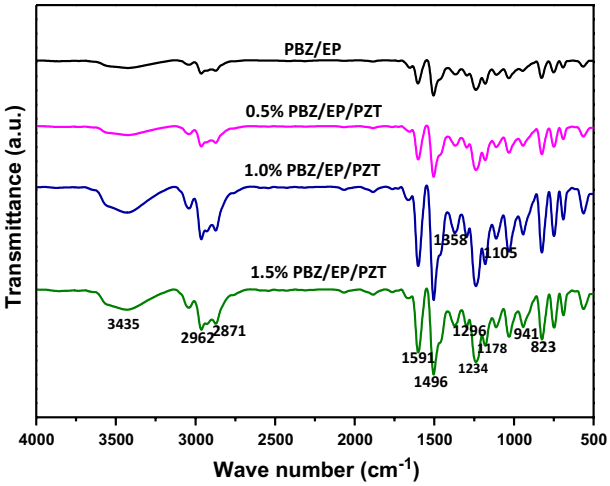

Fig. 1 FTIR spectra for neat PBZ/EP and PBZ/EP/PZT nanocomposites

P–O–(Ph) band [35]. From the figure, the disappearance of peaks at 937 cm^{-1} (for glycidyl groups present in DGEBA epoxy), 1520 cm^{-1} for trisubstituted benzene ring and 947 cm^{-1} for oxazine ring, and appearance of new peaks at 1505 cm^{-1} represents the tetra-substituted benzene ring [22], 2962 cm^{-1} and 2871 cm^{-1} for symmetric and asymmetric aliphatic CH_2 groups and the broad peak at 3435 cm^{-1} corresponding to –OH becomes weak indicating that the DGEBA undergoes a complete curing reaction with BZ-a to form an inter-cross-linked network structure.

Thermal resistance and stability of the nanocomposites

The thermal resistance is one of the most important properties of thermosets because it establishes the service environment for the epoxy-based functional materials. Usually, the glass transition temperature (T_g) represents the thermal resistance of the thermosets, which indicates the suitability of the material for specific applications. Therefore, it is very important for thermoset to achieve a high T_g using appropriate molecular structure. The T_g's of PZT fiber-reinforced PBZ/EP thermosets were determined by DSC, and the data obtained are presented in Table 1. From the data, observed that all the thermosets show higher values of T_g when compared with that of the conventional epoxy [28, 37]. The values of T_g of neat PBZ/EP and PZT incorporated PBZ/EP are 171, 188, 195, and 208 °C, respectively (Fig. 2). The values of T_g are increased with increase in weight percentages of PZT nanofiber reinforced into PBZ/EP matrix. It is well known that glass transition is generally ascribed to the segmental motion of the polymeric networks, and the T_g is determined by the degree of freedom for the segmental motion, cross-linking and entanglement constraints, and the packing density of the segments. In this work, PZT fiber of varying weight percentages was incorporated into the backbone chain of the hybrid PBZ/EP matrix to improve the network structure in addition to the presence of sterically hindered

Table 1 Thermal, flame resistant, and dielectric properties of neat PBZ/EP and PBZ/EP/PZT nanocomposites

Sample code	*T*g (°C)	T_d 5% weight loss (°C)	T_d 10% weight loss (°C)	Char yield at 800 °C	LOI	UL-94	Dielectric constant at 1 MHz		Dielectric loss at 1 MHz	
							30 °C	200 °C	30 °C	200 °C
PBZ [22]	180	312	–	36	32	–	3.48	–	–	–
EP [40]	162	–	308	12	23	–	4.30	–	–	–
PBZ/EP	171	270	327	21	26	–	4.72	3.63	0.012	0.0165
0.5 wt% PBZ/EP/PZT	188	297	345	37	32	V-1	4.45	2.99	0.010	0.0044
1.0 wt% PBZ/EP/PZT	195	311	354	38	33	V-0	3.95	2.75	0.009	0.0024
1.5 wt% PBZ/EP/PZT	208	328	362	41	35	V-0	3.42	2.47	0.008	0.0007

T_d–Degradation temperature

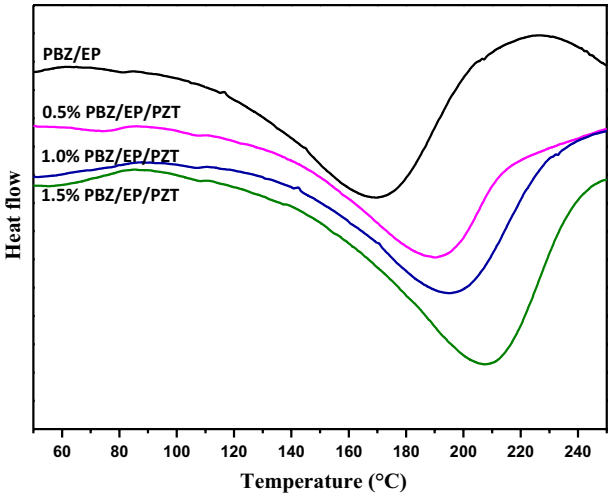

Fig. 2 DSC thermogram for neat PBZ/EP and PBZ/EP/PZT nanocomposites

aromatic substituents on the phosphazene ring to enhance the value of T_g. Thus, the values of T_g of cyclotriphosphazene-linked PBZ/EP are increased as a result of the retarded segmental motion. In addition, the abundant rigid aromatic rings and sulfone groups in the PZT fiber can further increase the rigidity of the resulting hybrid nanocomposites, which in turn contributes to the enhanced value of T_g.

The thermal stability of PZT fiber-incorporated PBZ/EP thermosets was investigated by TGA under a nitrogen atmosphere. The TGA thermogram of PBZ/EP/PZT and the data resulted are shown in Fig. 3, and the details of the thermal analysis are presented in Table 1. From the TGA traces of PBZ/EP/PZT, it was observed that

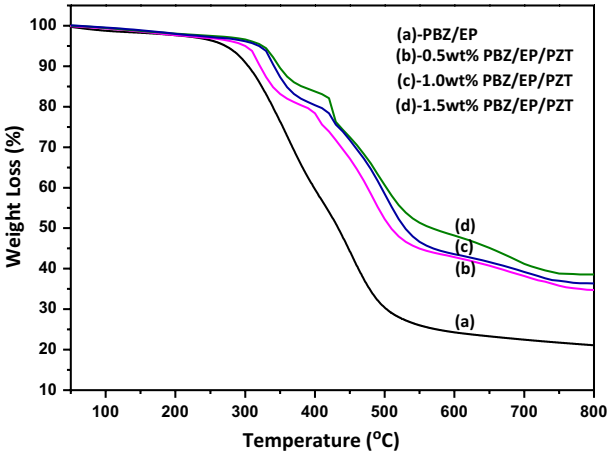

Fig. 3 TGA thermogram for **a** neat, **b** 0.5 **c** 1.0 and **d** 1.5 wt% of PBZ/EP/PZT nanocomposites (char yield of the a–d is 21, 37, 38 and 41%, respectively)

there was a two-stage thermal decomposition occurred due to the nature of constituents while PBZ/EP shows single-stage degradation. The first stage of thermal degradation is caused by the hydrocarbon segments of the thermoset, and the second stage is attributed to the decomposition of the major backbones of polymeric networks due to their higher thermal stability. The TGA results also demonstrate that the initial degradation temperatures (T_d) of all the thermosets corresponding to 5 wt% weight loss (T_d5) and 10 wt% weight loss (T_d10) are in the ranges of 270–328 °C and 308–362 °C, respectively. It was also noticed that the major decomposition occurs beyond 400 °C which indicate that the PZT fiber-reinforced PBZ/EP nanocomposites have good thermal stability. This may be due to the decomposition of the phosphorus and nitrogen groups in the PZT fiber that triggered the formation of the phosphorus- and nitrogen-rich char to hinder further decomposition of the PBZ/EP. Also, PZT fiber with many phenolic groups participated to increase the high cross-linking density of PBZ/EP. From the data presented in Table 1, it can be seen that the neat PBZ/EP shows the char yield of 21 wt%, whereas that of PZT fiber-reinforced PBZ/EP (0.5, 1.0, and 1.5 wt%) shows 37, 38, and 41%, respectively. An improvement of such higher char yields may be explained by the highly thermally stable phosphazene rings (phosphorus and nitrogen group in the PZT) in the PBZ/EP, which promotes the char formation during pyrolysis. The formation of phosphorus- and nitrogen-rich char in the decomposition of PBZ/EP/PZT not only increased the degradation temperature but also increased the high char yield. On the basis of these results, it can be concluded that the heat resistance of PZT incorporated PBZ/EP nanocomposites is superior to that of other known phosphorus-containing epoxy resins that have been reported [39].

Flammability characteristics of the nanocomposites

The UL-94 burning experiment is most important to assess the burning behavior of materials and is a widely used method for determining the upward burning characteristics of PBZ/EP/PZT nanocomposites. The UL-94 burning test results of the PBZ/EP/PZT nanocomposites are presented in Table 1. As expected, 0.5 wt% PBZ/EP/PZT attained the V-1 rating and that of 1.0 and 1.5 wt% PBZ/EP/PZT nanocomposites are V-0 classification, whereas the neat PBZ/EP matrix is burning in a UL-94 test. It is surprisingly noticed that the PZT fiber-incorporated nanocomposites did not exhibit an aggressive combustion during the tests, and there were no flaming drips which were observed as well. One of the fascinating characteristics of combustion is that most of the testing bars just combusted slightly with a small blaze and quenched within 5 s when the flame agitator was removed during the vertical burning test, indicating a self-extinguishable behavior. At the end of burning experiments, the surfaces of these nanocomposites were covered with an expanded char network, indicating that the thermosets formed an effective char which was able to prevent the heat transfer and flame spread during combustion. These results provide an evidence for non-flammability of the PZT fiber-reinforced PBZ/EP nanocomposites.

The limiting oxygen index (LOI) is considered as another important method used to quantify the flame-retardant behavior of organic polymer matrices. LOI represents the lowest environmental oxygen required for sustaining a flame. The oxygen volume content of the ambient atmosphere is about 21%. Therefore, a material exhibiting an LOI value above 21% might show flame-retardant properties [40]. The oxidized layer serves as a barrier against heat and oxygen diffusion, which contributes to the flame-retardant behavior to polymers in the high-temperature region and also gives high char yields. It has also been reported that a high char yield leads to high flame retardancy.

In the present study, the flame-retardant behavior of PBZ/EP and the varying weight percentages of PZT fiber-reinforced hybrid nanocomposites were analyzed. The values obtained are presented in Table 1; the values are found to be in the range of 26–35. Furthermore, the behavior of flame retardancy increased as the concentration of PZT fiber was increased. Burning behavior was correlated with the cross-link density of the matrix; i.e., with increasing cross-link density, the flammability resistance increased due to the formation of higher char. Thus, it can be concluded that the developed PBZ/EP/PZT can be used as better flame-retardant materials, where a high-performance application is required.

Analysis of residual char of the nanocomposites

It was considered that the residual chars formed during combustion can give some important information regarding the inherent flammability characteristics of a polymeric material, and they also reflect the fire-resistant mechanisms to some extent. Furthermore, the physical structure of the charring layer also plays a very important role in the performance of flame retardancy. Therefore, the morphology of the residual chars obtained from UL-94 burning tests was investigated by SEM. Figure 4 illustrates the SEM images of these residual chars. As shown by Fig. 4b–d, the outline of these residual chars exhibited some irregular-shaped bulk and the inside of the char shows a multiporous structure according to the magnified micrographs of each sample, indicating a typical morphology after the intumescent char formation. Additionally, all the residual chars observed have displayed a very gassy surface with a few pores breaking through. These charred layers formed during the combustion provide a rigid and compact texture in nature, and there are lots of integrated honeycomb pores inside. Such a structural form favors the temperature grads in the char layer and protects the matrix inside. Therefore, it is concluded that the thermo-oxidative reaction of cyclotriphosphazene moieties enhances the char formation during combustion, results in a protective char layer formed on the surface of PBZ/EP, which serves as a barrier against heat and oxygen diffusion, and consequently, the flame retardancy of the nanocomposites was improved significantly. Moreover, the multiporous structure of residual char also depends on the other factors such as the condition of curing, gases released during combustion, the composition, and structural feature of PBZ/EP/PZT nanocomposites.

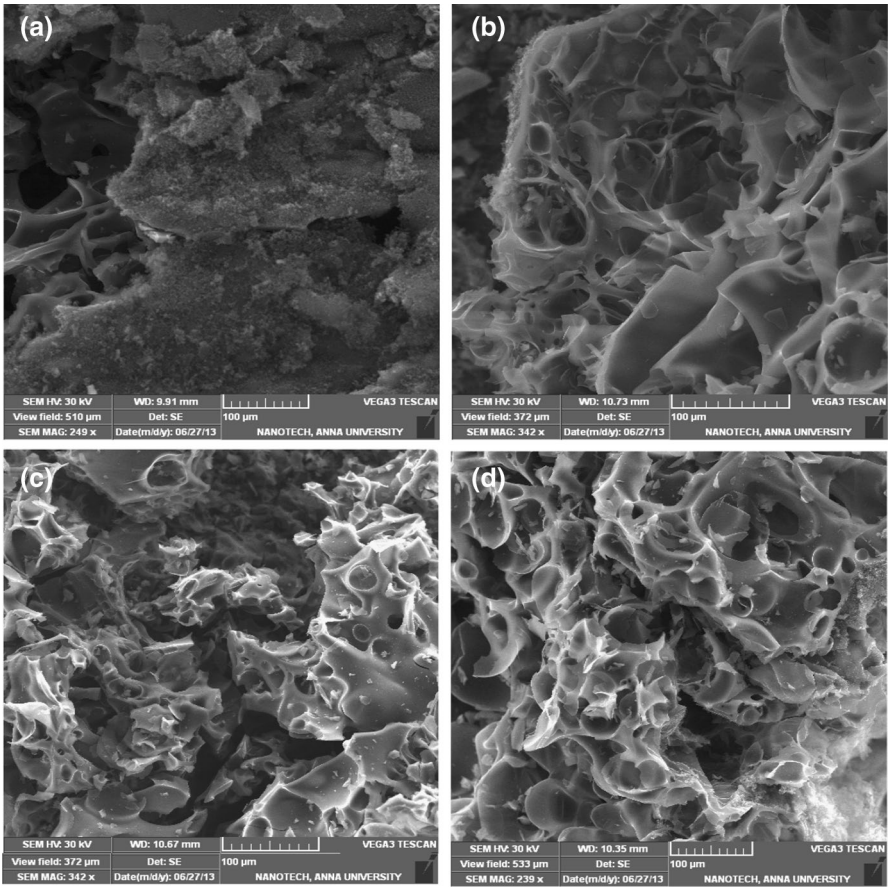

Fig. 4 SEM morphology of the residual chars of **a** neat, **b** 0.5 **c** 1.0 and **d** 1.5 wt% of PBZ/EP/PZT nanocomposites

Dielectric constant of the nanocomposites at varying temperatures

The variation of values of dielectric constant with temperature at 1 MHz is shown in Fig. 5. The values of dielectric constant are decreased with increasing the temperature. The temperature coefficient of dielectric constant values with regard to the percentage weight concentration of PZT fibers is 0.006, 0.008, 0.0078, and 0.0078 for 0, 0.5, 1.0, and 1.5 wt%, respectively. From the values, it can be ascertained that the composite samples exhibit stable dielectric behavior with regard to variation in temperature. The dielectric properties of a polymer are determined by the free volume, charge distribution and also by the statistical thermal motion of its polar group. In the case of PBZ/EP/PZT nanocomposites, the values of dielectric constant are 4.4, 4.0, and 3.4 with an increasing PZT fiber loading level of 0.5, 1.0, and 1.5 wt%, respectively, for 1 MHZ at 30 °C, when the temperature was raised to 200 °C the values of dielectric constant are reduced to 2.9, 2.7, and 2.4, respectively. The

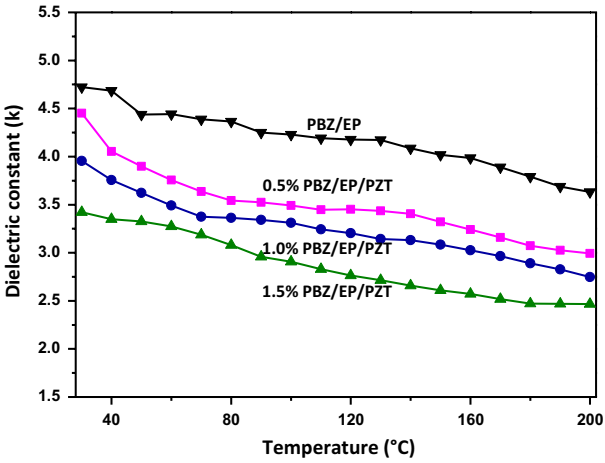

Fig. 5 Dielectric constant with various temperatures for neat PBZ/EP and PBZ/EP/PZT nanocomposites

reduction in the value of dielectric constant may be explained due to an enhanced free volume and also to the certain extent due to the influencing effect of PZT fiber.

The value of dielectric losses of neat PBZ/EP is marginal at 30–140 °C, and above 140 °C, the value of dielectric losses is significant and this supports the concept of free volume theory according to which the molecular mobility near T_g depends mainly on free volume. In the glassy state below T_g, the free volume will be frozen in and remain fixed. As the temperature increases, the glassy state will expand due to the increase in free volume in the molecular system, which results from the changing irrational amplitude of bound distances. This leads to the maximum dielectric loss at and above T_g for neat PBZ/EP (Fig. 6). In the case of PZT

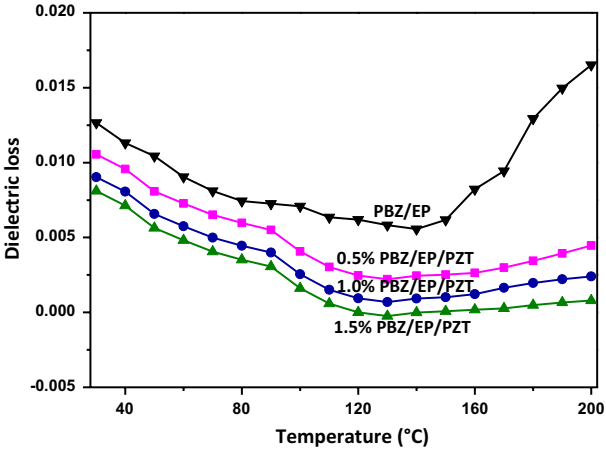

Fig. 6 Dielectric loss with various temperatures for neat PBZ/EP and PBZ/EP/PZT nanocomposites

fiber-reinforced PBZ/EP nanocomposites, the dielectric loss was reduced significantly with increasing temperature and the reverse trend in the case of dielectric loss was observed above 170 °C, due to an increase in T_g's and is interpreted on the basis of the nanoreinforcement of PZT fibers, which could restrict the motions of macromolecular chains. In the present study, it was also noticed that the enhancement in the value of *T*g is not only ascribed to the nanoreinforcement of PZT fiber but also attributed to the additional cross-linking of the nanocomposites resulting from the inter-component reaction between PZT and PBZ/EP.

Morphology

Figure 7a–c shows the TEM images of 0.5, 1.0, and 1.5 wt% of PBZ/EP/PZT nanocomposites, respectively. From the figure, it can be ascertained that the PZT nanofibers are flexible and are about 100 nm in diameter and the PZT fibers are

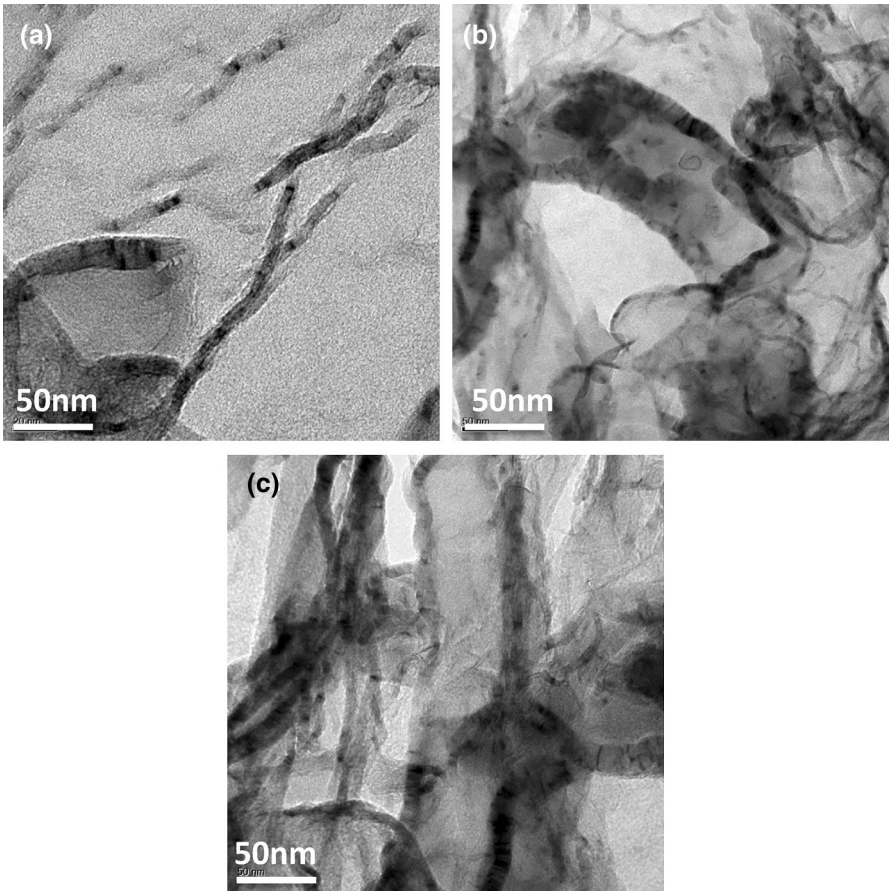

Fig. 7 TEM images of **a** 0.5, **b** 1.0, and **c** 1.5 wt% of PBZ/EP/PZT nanocomposites

homogeneously dispersed within the PBZ/EP matrix. From the TEM images, it is concluded that the PZT fiber was completely and uniformly dispersed within the PBZ/EP matrix. This is due to the strong covalent interactions resulted between the PZT fiber and the PBZ/EP matrix. The nanometer level dispersion of PZT fiber in the PBZ/EP matrix also influences the thermal and electrical properties of the resulting PBZ/EP/PZT nanocomposites.

Conclusion

Flame-retardant PBZ/EP/PZT hybrid nanocomposites have been successfully developed with varying weight percentages (0.0, 0.5, 1.0 and 1.5%) of PZT fiber reinforced with PBZ/EP matrix through thermal curing. Data resulted from DSC and TGA analysis indicate that the PBZ/EP/PZT possess the higher values of Tg as well as char yield and higher thermal stability than that of neat PBZ/EP. Furthermore, the PBZ/EP/PZT nanocomposites possess V-0 classification from the UL-94 test, indicating an excellent flame-retardant behavior. This is attributed to the structural feature of PBZ/EP covalently bonded with PZT fiber. The presence of such a unique combination of phosphorus and nitrogen in the PZT contributes to a good flame-retardant behavior. The compatibility between PZT fiber and PBZ/EP was confirmed by TEM analysis. In addition, the nanocomposites based on the PZT fiber exhibited lower values of dielectric constant and dielectric loss over a wide range of temperatures indicating its suitability for effective and thermally stable flame-retardant dielectric materials for microelectronic applications.

References

1. Alexander BM, Jeffrey WG (2013) An overview of flame retardancy of polymeric materials: application, technology, and future directions. Fire Mater 37:259–279
2. Blomqvist P, Rosell L, Simonson M (2004) Emissions from fires part i: fire retarded and non-fire retarded TV-sets. Fire Technol 40:39–58
3. Kiliaris P, Papaspyrides CD (2010) Polymer/layered silicate (clay) nanocomposites: an overview of flame retardancy. Prog Polym Sci 35:902–958
4. Liao SH, Liu PO, Hsiao MC, Teng CC, Wang CA, Ger MD, Chiang CL (2012) One-step reduction and functionalization of graphene oxide with phosphorus-based compound to produce flame-retardant epoxy nanocomposite. Ind Eng Chem Res 51:4573–4581
5. Xiaodong Q, Lei S, Bin Y, Bibo W, Bihe Y, Yongqian S, Yuan H, Richard KKY (2013) Novel organic–inorganic flame retardants containing exfoliated graphene: preparation and their performance on the flame retardancy of epoxy resins. J Mater Chem A 1:6822–6830
6. Weil ED, Levchik SV (2004) A Review of current flame retardant systems for epoxy resins. J Fire Sci 22:25–40
7. Xin W, Lei S, Hongyu Y, Weiyi X, Baljinder K, Yuan H (2012) Simultaneous reduction and surface functionalization of graphene oxide with POSS for reducing fire hazards in epoxy composites. J Mater Chem 22:22037–22043
8. Jin FL, Li X, Park SJ (2015) Synthesis and application of epoxy resins: A review. J Ind Eng Chem 29:1–11
9. Vidil T, Tournilhac F, Musso S, Robisson A, Leibler L (2016) Control of reactions and network structures of epoxy thermosets. Prog Polym Sci 62:126–179

10. Sponton M, Lligadas G, Ronda JC, Galià M, Cádiz V (2009) Development of a DOPO-containing benzoxazine and its high-performance flame retardant copolybenzoxazines. Polym Degrad Stab 94:1693–1699
11. Artner J, Ciesielski M, Walter O, Doring M, Perez RM, Sandler JKW, Altstädt V, Schartel B (2008) A novel DOPO-based diamine as hardener and flame retardant for epoxy resin systems. Macromol Mater Eng 293:503–514
12. Hongbo G, Jiang G, Qingliang H, Sruthi T, Zhang X, Yan X, Huang Y, Henry AC, Wei S, Zhanhu G (2013) Flame-retardant epoxy resin nanocomposites reinforced with polyaniline-stabilized silica nanoparticles. Ind Eng Chem Res 52:7718–7728
13. Gao M, Wu W, Yan Y (2009) Thermal degradation and flame retardancy of epoxy resins containing intumescent flame retardant. J Therm Anal Calorim 95:605–608
14. Gouri ME, Bachiri AE, Hegazi SE, Rafik M, Harfi AE (2009) Thermal degradation of a reactive flame retardant based on cyclotriphosphazene and its blend with DGEBA epoxy resin. Polym Degrad Stab 94:2101–2106
15. Wang X, Zhang Q (2004) Synthesis, characterization, and cure properties of phosphorus-containing epoxy resins for flame retardance. Eur Polym J 40:385–395
16. Wang X, Hu Y, Song L, Xing W, Lu H, Lv P, Jie G (2010) Flame retardancy and thermal degradation mechanism of epoxy resin composites based on a DOPO substituted organophosphorus oligomer. Polymer 51:2435–2445
17. Wang X, Song L, Xing W, Lu H, Hu Y (2011) A effective flame retardant for epoxy resins based on poly(DOPO substituted dihydroxyl phenyl pentaerythritol diphosphonate). Mater Chem Phys 125:536–541
18. Wang X, Zhou S, Xing W, Yu B, Feng X, Song L, Hu Y (2013) Self-assembly of Ni–Fe layered double hydroxide/graphene hybrids for reducing fire hazard in epoxy composites. J Mater Chem A 1:4383–4390
19. Hann JH, Chi YL, Chun SW (2008) Flame retardancy and dielectric properties of dicyclopentadiene-based benzoxazine cured with a phosphorus-containing phenolic resin. J Appl Polym Sci 110:2413–2423
20. Takeichi T, Kawauchi T, Agag T (2008) High performance polybenzoxazines as a novel type of phenolic resin. Polym J 40:1121–1131
21. Ishida H, Allen DJ (1996) Physical and mechanical characterization of near-zero shrinkage polybenzoxazines. J Polym Sci B Polym Phys 34:1019–1030
22. Ghosh NN, Kiskan B, Yagci Y (2007) Polybenzoxazines-New high performance thermosetting resins: synthesis and properties. Prog Polym Sci 32:1344–1391
23. Agag T, Takeichi T (2003) Synthesis and characterization of novel benzoxazine monomers containing allyl groups and their high performance thermosets. Macromolecules 36:6010–6017
24. Vengatesan MR, Devaraju S, Dinakaran K, Alagar M (2012) SBA-15 filled polybenzoxazine nanocomposites for low-k dielectric applications. J Mater Chem 22:7559–7566
25. Ishida H, Froimowicz P (2017) Advanced and emerging polybenzoxazine science and technology. John Fedor publisher, Elsevier, Washington DC
26. Allcock HR (2013) Chemistry and applications of polyphosphazenes. Wiley-Interscience, Hoboken, NJ
27. Allen CW (1993) The use of phosphazenes as fire resistant materials. J Fire Sci 11:320–328
28. Bai Y, Wang X, Wu D (2012) Novel cyclolinear cyclotriphosphazene-linked epoxy resin for halogen-free fire resistance: synthesis, characterization, and flammability characteristics. Ind Eng Chem Res 51:15064–15074
29. Lim H, Chang JY (2010) Thermally stable and flame retardant low dielectric polymers based on cyclotriphosphazenes. J Mater Chem 20:749–754
30. Wu X, Zhou Y, Liu SZ, Guo YA, Qiu JJ, Liu CM (2011) Highly branched benzoxazine monomer based on cyclotriphosphazene: synthesis and properties of the monomer and polybenzoxazines. Polymer 52:1004–1012
31. Zhao S, He M, Xu J, Ma H (2017) Synthesis of a functionalised phosphazene-containing nanotube/epoxy nanocomposite with enhanced flame retardancy. Micro Nano Lett 12:401–403
32. Qiu S, Wang X, Yu B, Feng X, Mu X, Yuen RKK, Hu Y (2017) Flame-retardant-wrapped polyphosphazene nanotubes: a novel strategy for enhancing the flame retardancy and smoke toxicity suppression of epoxy resins. J Hazard Mater 325:327–339

33. Qu T, Yang N, Houb J, Li G, Yao Y, Zhang Q, He L, Wu D, Qu X (2017) Flame retarding epoxy composites with poly(phosphazene-co-bisphenol A)-coated boron nitride to improve thermal conductivity and thermal stability. RSC Adv 7:6140–6151
34. Li S, Qiu S, Yu B, Tang G, Xing W, Hu Y (2016) POSS-functionalized polyphosphazene nanotube: preparation and effective reinforcement on UV-curable epoxy acrylate nanocomposite coatings. RSC Adv 6:3025–3031
35. Gu X, Huang X, Wei H, Tang X (2011) Synthesis of novel epoxy-group modified phosphazene-containing nanotube and its reinforcing effect in epoxy resin. Eur Polym J 47:903–910
36. Lu SY, Hamerton I (2002) Recent developments in the chemistry of halogen-free flame retardant polymers. Prog Polym Sci 27:1661–1712
37. Espinosa MA, Galia M, Cadiz V (2004) Novel phosphorilated flame retardant thermosets:epoxy–benzoxazine–novolac systems. Polymer 45:6103–6109
38. Lin CH, Cai SX, Leu TS, Hwang TY, Lee HH (2006) Synthesis and properties of flame-retardant benzoxazines by three approaches. J Polym Sci A Polym Chem 44:3454–3468
39. Zhang W, Li X, Yang R (2011) Pyrolysis and fire behaviour of epoxy resin composites based on a phosphorus-containing polyhedral oligomeric silsesquioxane (DOPO-POSS). Polym Degrad Stab 96:1821–1832
40. Devaraju S, Vengatesan MR, Selvi M, Song JK, Alagar M (2013) Hyper branched polysiloxane-based diglycidyl ether of bisphenol a epoxy composite for low k dielectric application. Polym Comp 34:904–911

Affiliations

M. Selvi[1] · S. Devaraju[2] · M. Alagar[3]

[1] Polymer Composite Lab, Department of Chemical Engineering, Anna University, Chennai 600 025, India

[2] Polymer Composites Lab, Division of Chemistry, Department of Science and Humanities, Vignan's Foundation for Science, Technology and Research (VFSTR), Vadlamudi, Guntur 522 213, India

[3] Centre of Excellence for Advanced Materials, Manufacturing, Processing and Characterisation (CoExAMMPC), Vignan's Foundation for Science, Technology and Research (VFSTR), Vadlamudi, Guntur 522 213, India